On the Nature of the Ultrarelativistic Prompt Emission (UPE) Phase of GRB 190114C and GRB 180720B

R. Moradi

ICRANet, ICRA-Sapienza University

J. Rueda, R. Ruffini, Lian Li, C. Bianco, S. Campion, C. Cerubini, S. Filippi, Y. Wang, S. Xue, F. Rastegarnia

Gamma Ray bursts are

Extremely energetic explosions!

- The most energetic sources in the universe!
- They produce energy equivalent to $\sim$1 solar mass in 1-100 second $\rightarrow\sim$ 10^{54} erg!
- if explosion $< 2s \rightarrow$ SHORT GRB.
- if explosion $> 2s \rightarrow$ LONG GRB.
- $\sim$ 10^{38} Tons of TNT explosion! in some seconds!

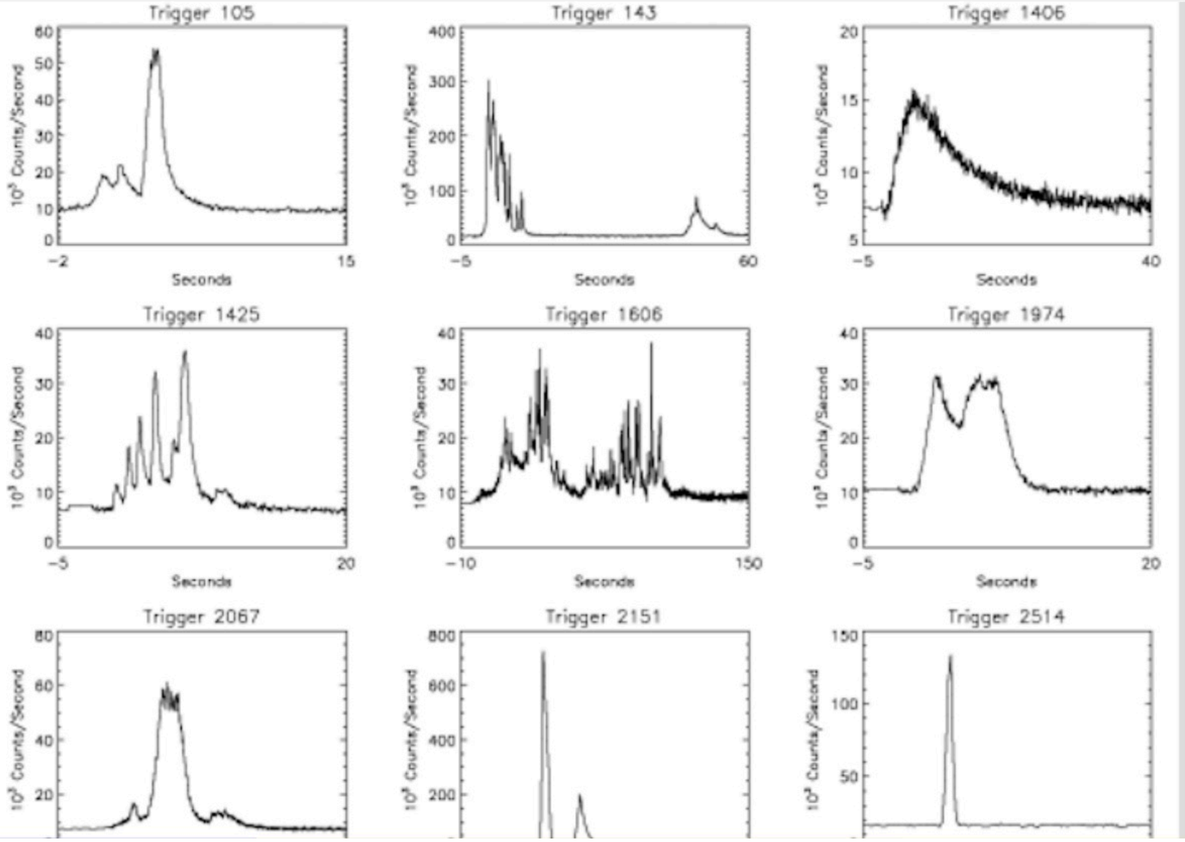

What are the numbers associated with GRBs?

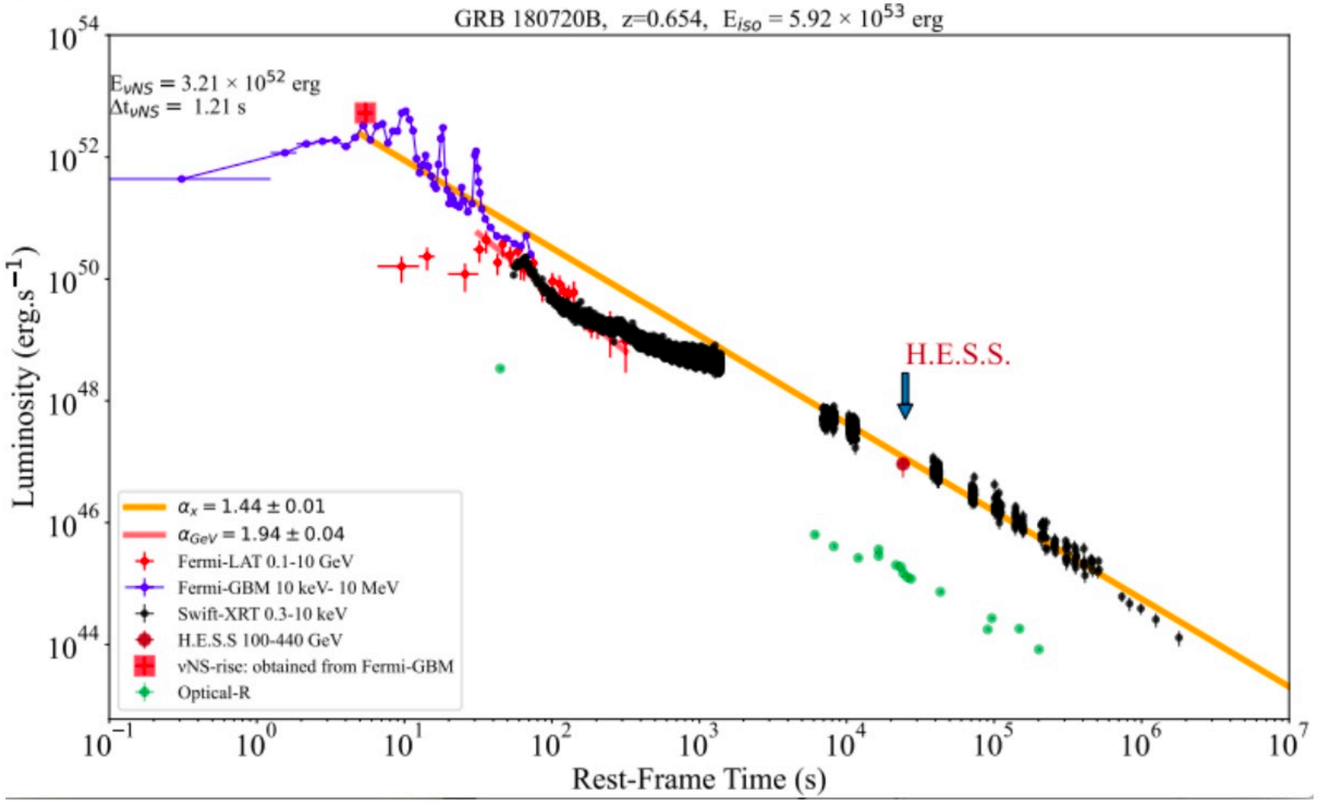

- 180720B
- 18 $\rightarrow$ 2018
- 07 $\rightarrow$ July
- 20 $\rightarrow$ day 20
- B $\rightarrow$ more than one GRB a day!

GRB 190114C As Binary driven HyperNova of type I (BdHN I)

Moradi, Rueda, Ruffini, Li, et al., PRD 104, 063043 (2021).

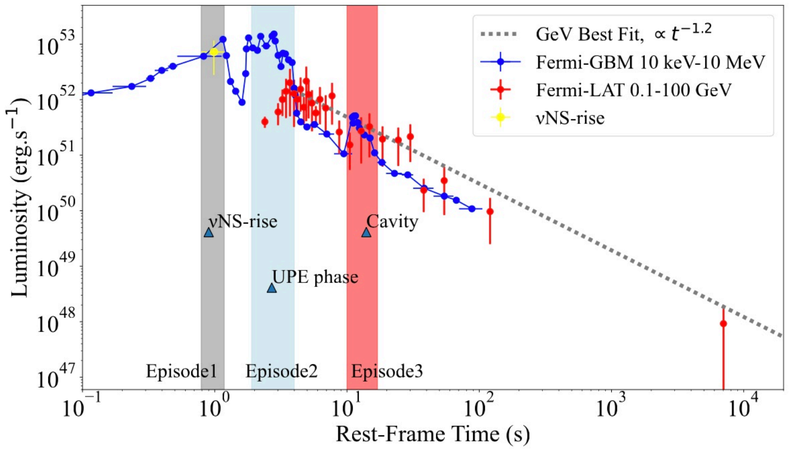

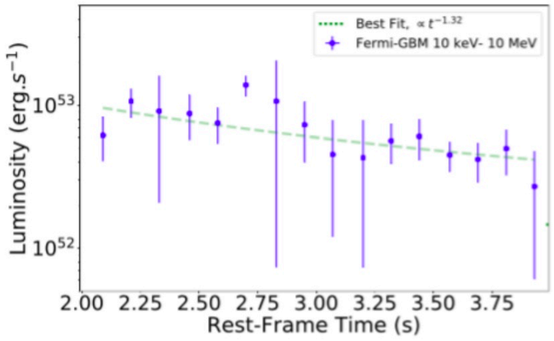

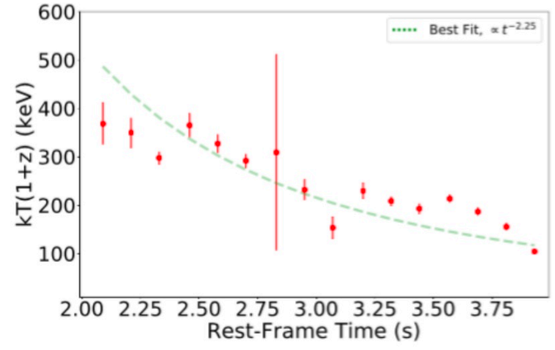

t_1~t_2 (a) Observation (1)	t_1~t_2 (a) Rest (2)	S (3)	α (keV) (4)	E_c (keV) (5)	kT (6)	-log[posterior]/[AIC/BIC] (10^{-6}) (erg cm^{-2} s^{-1}) (7)	F_{BB} (10^{-6}) (erg cm^{-2} s^{-1}) (8)	F_{Total} (9)	F_{ratio} (10)	E_{Total} (erg) Rest (11)
2.700~5.500	1.896~3.862	418.62	$-0.71^{+0.02}_{-0.02}$	$717.6^{+25.4}_{-25.4}$	$159.0^{+3.6}_{-3.6}$	-3344/6697/6719	$22.49^{+0.21}_{-0.21}$	$111.16^{+11.60}_{-10.40}$	0.20	$1.50e+53$
2.700~4.100	1.896~2.879	296.60	$-0.51^{+0.02}_{-0.02}$	$696.6^{+32.4}_{-32.4}$	$209.7^{+5.1}_{-5.1}$	-2675/5360/5381	$24.67^{+0.36}_{-0.36}$	$142.50^{+21.00}_{-21.00}$	0.17	$9.64e+52$
4.100~5.500	2.879~3.862	318.07	$-0.90^{+0.02}_{-0.02}$	$639.3^{+31.9}_{-31.6}$	$130.6^{+3.5}_{-3.5}$	-2529/5069/5090	$25.55^{+0.37}_{-0.37}$	$80.98^{+9.64}_{-8.67}$	0.32	$5.48e+52$
2.700~3.400	1.896~2.388	204.30	$-0.59^{+0.03}_{-0.03}$	$724.7^{+65.5}_{-65.5}$	$220.0^{+7.2}_{-7.2}$	-1882/3774/3796	$18.55^{+0.40}_{-0.40}$	$123.96^{+29.20}_{-25.20}$	0.15	$4.19e+52$
3.400~4.100	2.388~2.879	225.88	$-0.46^{+0.04}_{-0.04}$	$699.8^{+47.8}_{-48.3}$	$196.7^{+6.9}_{-6.7}$	-2032/4074/4095	$31.78^{+0.60}_{-0.60}$	$161.40^{+47.10}_{-32.40}$	0.20	$5.46e+52$
4.100~4.800	2.879~3.371	233.97	$-0.84^{+0.03}_{-0.03}$	$608.1^{+42.1}_{-42.1}$	$130.4^{+5.7}_{-5.7}$	-1880/3770/3792	$23.94^{+0.80}_{-0.80}$	$85.37^{+14.83}_{-11.40}$	0.28	$2.89e+52$
4.800~5.500	3.371~3.862	227.90	$-0.96^{+0.03}_{-0.03}$	$679.5^{+49.1}_{-49.7}$	$130.6^{+5.1}_{-5.1}$	-1809/3628/3649	$27.18^{+0.72}_{-0.72}$	$78.20^{+11.40}_{-9.06}$	0.35	$2.65e+52$
2.700~3.050	1.896~2.142	148.59	$-0.59^{+0.03}_{-0.03}$	$547.7^{+44.2}_{-44.2}$	$240.4^{+9.2}_{-9.2}$	-1187/2384/2406	$19.67^{+0.68}_{-0.68}$	$103.20^{+80.80}_{-29.20}$	0.19	$1.75e+52$
3.050~3.400	2.142~2.388	145.04	$-0.60^{+0.04}_{-0.04}$	$965.2^{+80.1}_{-80.1}$	$203.5^{+10.8}_{-10.8}$	-1320/2650/2671	$22.87^{+0.88}_{-0.88}$	$152.00^{+21.00}_{-21.00}$	0.15	$2.57e+52$
3.400~3.750	2.388~2.633	134.60	$-0.63^{+0.04}_{-0.04}$	$885.7^{+70.9}_{-71.1}$	$240.6^{+12.5}_{-12.4}$	-1224/2458/2480	$41.02^{+1.39}_{-1.39}$	$129.10^{+52.40}_{-31.70}$	0.32	$2.18e+52$
3.750~4.100	2.633~2.879	187.77	$-0.35^{+0.05}_{-0.06}$	$607.8^{+60.1}_{-60.1}$	$151.5^{+14.2}_{-14.2}$	-1428/2866/2887	$23.92^{+0.40}_{-0.40}$	$192.00^{+60.30}_{-60.30}$	0.12	$3.25e+52$
4.100~4.450	2.879~3.123	171.81	$-0.69^{+0.04}_{-0.04}$	$515.9^{+43.6}_{-43.6}$	$117.8^{+5.0}_{-5.0}$	-1271/2552/2573	$19.19^{+0.80}_{-0.80}$	$92.71^{+27.69}_{-22.43}$	0.21	$1.57e+52$
4.450~4.800	3.125~3.371	230.14	$-0.98^{+0.04}_{-0.04}$	$702.0^{+78.2}_{-78.2}$	$141.3^{+5.8}_{-5.8}$	-1254/2518/2539	$26.76^{+0.47}_{-0.47}$	$80.73^{+14.95}_{-11.95}$	0.33	$1.37e+52$
4.800~5.150	3.371~3.617	166.30	$-0.97^{+0.04}_{-0.04}$	$685.1^{+69.4}_{-68.6}$	$140.8^{+5.6}_{-5.6}$	-1218/2447/2468	$31.83^{+0.85}_{-0.85}$	$82.51^{+15.02}_{-12.03}$	0.39	$1.40e+52$
5.150~5.500	3.617~3.862	161.51	$-0.95^{+0.04}_{-0.04}$	$692.2^{+79.1}_{-79.1}$	$120.0^{+5.0}_{-5.0}$	-1203/2416/2438	$23.19^{+0.38}_{-0.38}$	$73.57^{+12.83}_{-9.83}$	0.32	$1.24e+52$
2.700~2.875	1.896~2.019	117.09	$-0.58^{+0.05}_{-0.05}$	$470.5^{+74.4}_{-83.7}$	$261.4^{+19.3}_{-17.9}$	-640/1291/1311	$33.68^{+0.39}_{-0.39}$	$112.30^{+29.37}_{-25.73}$	0.30	$9.50e+51$
2.875~3.050	2.019~2.142	94.49	$-0.68^{+0.05}_{-0.05}$	$627.6^{+91.5}_{-91.5}$	$258.0^{+19.7}_{-19.7}$	-664/1337/1359	$28.45^{+0.33}_{-0.33}$	$98.14^{+26.64}_{-22.64}$	0.29	$8.30e+51$
3.050~3.225	2.142~2.265	106.62	$-0.59^{+0.03}_{-0.03}$	$957.1^{+94.1}_{-94.9}$	$245.3^{+27.5}_{-21.0}$	-768/1547/1568	$25.71^{+0.37}_{-0.37}$	$169.30^{+56.20}_{-31.60}$	0.15	$1.43e+52$
3.225~3.400	2.265~2.388	100.40	$-0.73^{+0.06}_{-0.06}$	$1275.9^{+209.9}_{-209.9}$	$208.6^{+9.1}_{-9.1}$	-669/1349/1369	$36.78^{+0.54}_{-0.54}$	$144.90^{+35.02}_{-34.50}$	0.25	$1.23e+52$
3.400~3.573	2.388~2.511	98.23	$-0.59^{+0.05}_{-0.05}$	$804.0^{+82.3}_{-82.3}$	$255.9^{+17.4}_{-17.4}$	-702/1414/1436	$42.19^{+0.43}_{-0.43}$	$139.30^{+35.60}_{-34.50}$	0.30	$1.18e+52$
3.573~3.750	2.511~2.633	93.84	$-0.65^{+0.04}_{-0.04}$	$916.3^{+67.7}_{-67.7}$	$229.9^{+15.9}_{-15.9}$	-730/147/1492	$39.25^{+0.37}_{-0.37}$	$119.50^{+34.40}_{-32.40}$	0.33	$1.01e+52$
3.750~3.925	2.633~2.756	126.63	$-0.51^{+0.02}_{-0.02}$	$960.9^{+80.9}_{-80.9}$	$204.6^{+10.0}_{-10.0}$	-808/1627/1648	$57.70^{+0.41}_{-0.41}$	$221.10^{+55.40}_{-51.50}$	0.26	$1.87e+52$
3.925~4.100	2.756~2.879	141.61	$-0.19^{+0.02}_{-0.02}$	$398.7^{+12.1}_{-12.1}$	$216.5^{+12.0}_{-12.0}$	-734/1479/1499	$0.02^{+0.23}_{-0.23}$	$170.20^{+12.08}_{-12.08}$	0.00	$1.44e+52$
4.100~4.275	2.879~3.002	122.91	$-0.54^{+0.06}_{-0.06}$	$474.1^{+46.2}_{-46.2}$	$162.6^{+14.9}_{-14.9}$	-758/1526/1547	$24.26^{+0.09}_{-0.09}$	$116.10^{+62.40}_{-35.12}$	0.21	$9.82e+51$
4.275~4.450	3.002~3.125	122.62	$-0.64^{+0.06}_{-0.06}$	$363.0^{+46.0}_{-46.0}$	$107.4^{+12.9}_{-12.9}$	-675/1360/1380	$9.04^{+0.47}_{-0.47}$	$72.20^{+19.08}_{-11.80}$	0.13	$6.11e+51$
4.450~4.625	3.125~3.248	111.94	$-1.04^{+0.05}_{-0.05}$	$640.0^{+108.5}_{-108.1}$	$161.0^{+10.8}_{-10.8}$	-640/1290/1310	$22.34^{+0.56}_{-0.56}$	$68.54^{+11.21}_{-11.21}$	0.33	$5.80e+51$
4.625~4.800	3.248~3.371	123.33	$-0.95^{+0.05}_{-0.05}$	$694.2^{+96.8}_{-96.8}$	$146.3^{+9.7}_{-9.7}$	-734/1477/1499	$35.59^{+0.47}_{-0.47}$	$89.91^{+27.69}_{-27.69}$	0.40	$7.60e+51$
4.800~4.975	3.371~3.494	129.65	$-0.85^{+0.05}_{-0.05}$	$564.5^{+71.9}_{-71.9}$	$133.3^{+7.6}_{-7.6}$	-744/1498/1519	$30.78^{+0.55}_{-0.55}$	$96.58^{+23.68}_{-21.02}$	0.32	$8.17e+51$
4.975~5.150	3.494~3.617	107.36	$-1.10^{+0.04}_{-0.04}$	$820.5^{+115.0}_{-111.2}$	$149.7^{+8.9}_{-8.8}$	-683/1376/1398	$32.76^{+0.99}_{-0.99}$	$71.57^{+16.74}_{-11.99}$	0.46	$6.05e+51$
5.150~5.325	3.617~3.739	108.96	$-1.04^{+0.05}_{-0.05}$	$765.2^{+118.9}_{-118.9}$	$130.9^{+5.8}_{-5.8}$	-697/1404/1426	$26.14^{+0.96}_{-0.96}$	$66.70^{+14.17}_{-14.17}$	0.39	$5.64e+51$
5.325~5.500	3.739~3.862	121.57	$-0.88^{+0.06}_{-0.06}$	$635.3^{+88.7}_{-92.0}$	$108.9^{+5.3}_{-5.4}$	-736/1483/1504	$20.90^{+0.51}_{-0.51}$	$79.48^{+24.02}_{-21.03}$	0.26	$6.72e+51$
5.500~5.675	3.862~3.985	111.83	$-1.00^{+0.08}_{-0.08}$	$437.7^{+82.2}_{-81.7}$	$73.2^{+2.9}_{-2.9}$	-587/1184/1205	$12.45^{+0.10}_{-0.10}$	$43.09^{+9.73}_{-8.46}$	0.29	$3.64e+51$

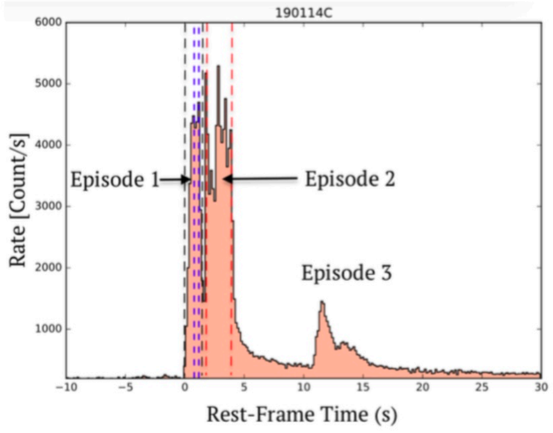

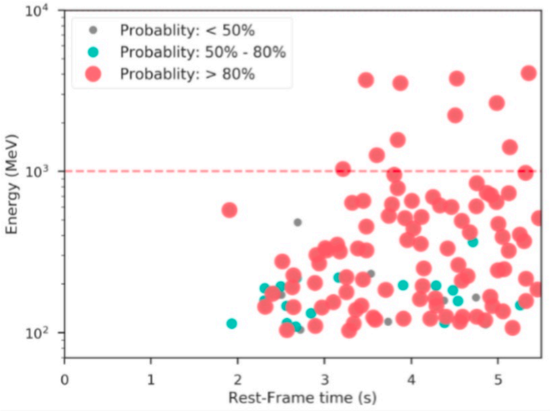

- At 20:57:02.63 UT on 14 January 2019, Fermi-GBM was triggered by GRB 190114C. . Following the 0.37 second at 20:57:03 UT on 14 January 2019, the Neil Gehrels Swift Burst Alert Telescope (BAT) was triggered as well by GRB 190114C.
- The Fermi-LAT had a boresight angle of 68 deg at the trigger time, the GRB remained in the field of view of Fermi-LAT for 150 seconds.
- Nordic Optical Telescope (NOT) announced by GCN23695 the redshift of 0.424.
- At time 15:29:54 GMT on January 15, 2019 we identified by GCN23715 this GRB as a BdHN I, and predicted that an optical SN should appear in the same location of the GRB within 18.8 ± 3.7 days, which indeed was confirmed by Melandri et al.
- This successful prediction and the following detection of TeV radiation by MAGIC have made GRB 190114C as a prototype which all the BdHN phases have been observed.

BdHN I includes three different components:

1. a CO core undergoing a SN explosion in presence of a binary NS companion;
2. an additional NS originating from the SN explosion indicated as a νNS (the newborn NS at the center of the SN), accreting the SN ejecta and giving origin to the afterglow;
3. the formation of the BH by the hypercritical accretion of the SN ejecta onto the NS reaching its critical mass. The newborn BH originates the GeV emission. Coincidence of these effect, the birth of BH and the onset of the GeV emission has been narrow down by our to 10^{-6} s.

Fryer, et al., ApJ 526, 152 (1999)
Bromberg, et al., ApJ 749, 110(2012)
Götberg, et al., AA 629, A134 (2019)

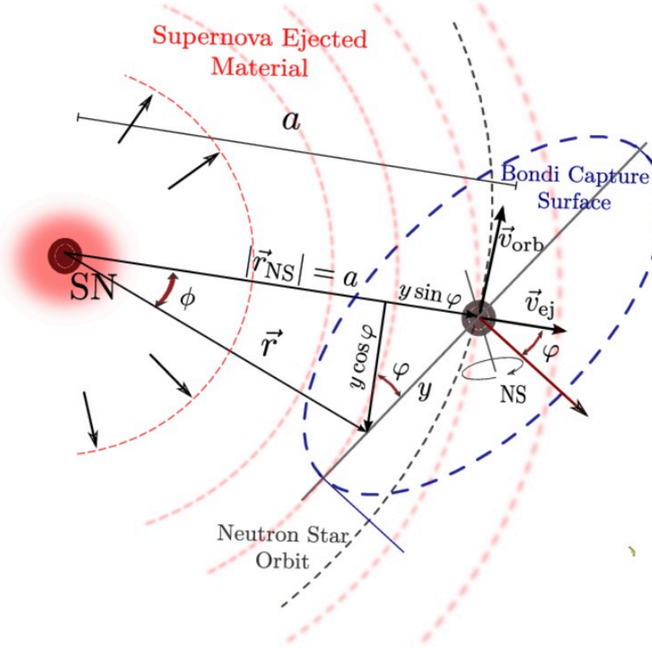

Rueda & Ruffini, ApJ 758, L7 (2012)
Becerra, et al., ApJ 812, 100 (2015)
Becerra, et al., ApJ 871, 14 (2019)

BdHN model in movies

The Correspondence 2016
By J. Tornatore

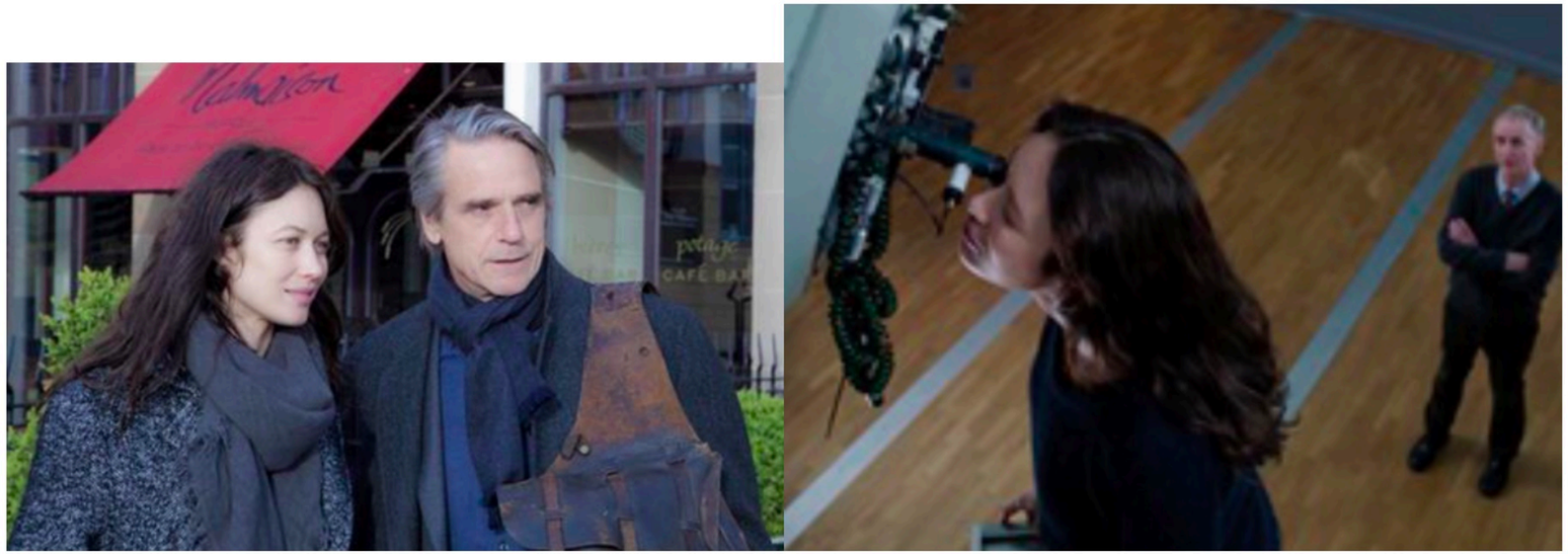

Olga Kurylenko and Jeremy Irons: The Correspondence

Black Hole

a) Wilson, J. R. 1975, in Annals of the New York Academy of Sciences

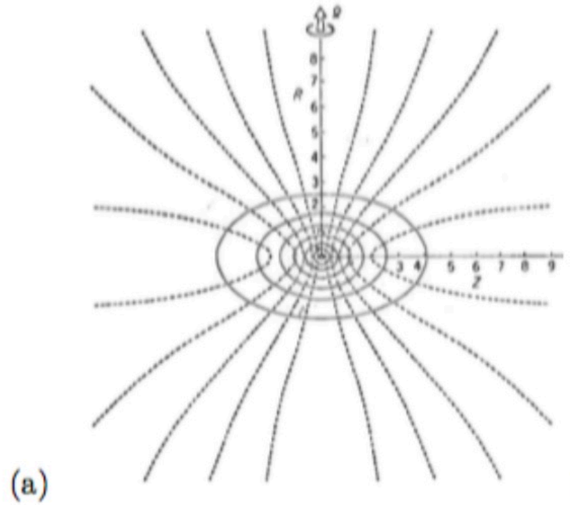

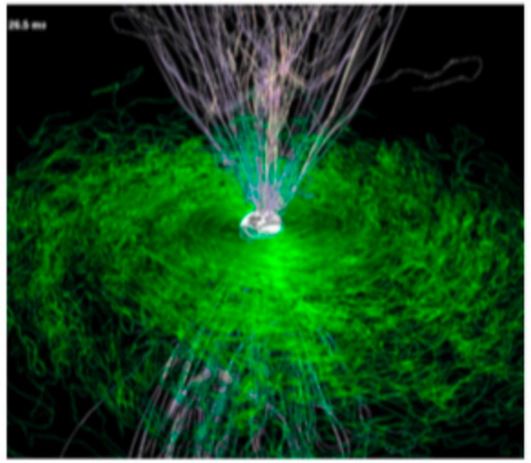

b) Rezzolla, L., Giacomazzo, B., Baiotti, L., et al. 2011, ApJL,732, L6

Kerr Metric in a uniform magnetic field

The Kerr space-time metric (geometric units will be considered), which is stationary and axisymmetric, in standard Boyer-Lindquist (BL) coordinates reads

$$\begin{aligned} ds^2 &= -\left(1-\frac{2Mr}{\Sigma}\right)dt^2 - \frac{4aMr\sin^2\theta}{\Sigma}dtd\phi + \frac{\Sigma}{\Delta}dr^2 \\ &+ \Sigma d\theta^2 + \left[r^2+a^2+\frac{2Mra^2\sin^2\theta}{\Sigma}\right]\sin^2\theta d\phi^2, \end{aligned}$$

where $\Sigma = r^2 + a^2\cos^2\theta$ and $\Delta = r^2 - 2Mr + a^2$. The (outer) event horizon is located at $r_+ = M + \sqrt{M^2 - a^2}$.

Accretion to NS -> BH formation+Magnetic field

Killing vectors and Maxwell field

$$\mathcal{L}_\zeta g_{\mu\nu} = \zeta_{\mu;\nu} + \zeta_{\nu;\mu}$$

- Papapetrou: Killing vector in vacuum space-time generates a solution of Maxwell's equations in that space-time.
- The solution of electromagnetic test-field which occurs when a stationary, axisymmetric black hole is placed in an originally uniform magnetic field of strength B_0 aligned along the symmetry axis of rotation of the black hole is
- $$\mathbf{F} = \frac{1}{2} B_0 (d\psi + \frac{2J}{M} d\eta)$$

  J: angular momentum, M: mass of the black hole, ψ: axial Killing vector, η: timelike Killing vector.

The electromagnetic field of the *inner engine* in the Carter's orthonormal tetrad is:

$$
\begin{aligned}
E_{\hat{r}} &= \frac{\hat{a}B_0}{\Sigma}\left[r\sin^2\theta - \frac{\hat{M}\left(\cos^2\theta+1\right)\left(r^2-\hat{a}^2\cos^2\theta\right)}{\Sigma}\right], \\
E_{\hat{\theta}} &= \frac{\hat{a}B_0}{\Sigma}\sin\theta\cos\theta\sqrt{\Delta}, \\
B_{\hat{r}} &= -\frac{B_0\cos\theta}{\Sigma}\left[-\frac{2\hat{a}^2\hat{M}r\left(\cos^2\theta+1\right)}{\Sigma}+\hat{a}^2+r^2\right], \\
B_{\hat{\theta}} &= \frac{B_0 r}{\Sigma}\sin\theta\sqrt{\Delta},
\end{aligned}
$$

where $\Sigma = r^2 + \hat{a}^2\cos^2\theta$, $\Delta = r^2 - 2\hat{M}r + \hat{a}^2$, $\hat{M} = GM/c^2$, $\hat{a} = a/c = J/(Mc)$, being M and J the mass and angular momentum of the Kerr BH. The (outer) event horizon is located at $r_+ = (\hat{M} + \sqrt{\hat{M}^2 - \hat{a}^2})$.

The inner engine

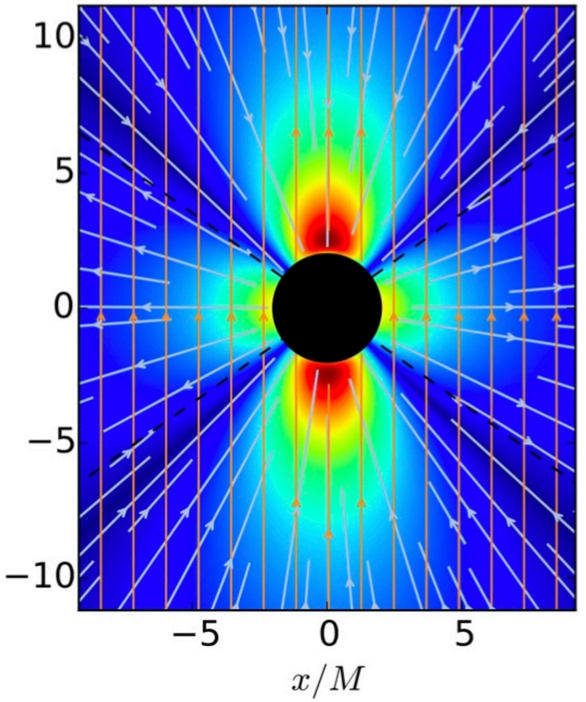

A&A 649, A75 (2021)
https://doi.org/10.1051/0004-6361/201937135

Astronomy & Astrophysics

The newborn black hole in GRB 191014C proves that it is alive

R. Moradi[1,2,3], J. A. Rueda[1,2,4,5,6], R. Ruffini[1,2,7], and Y. Wang[1,2,3]

[1] ICRANet, Piazza della Repubblica 10, 65122 Pescara, Italy
e-mail: rahim.moradi@icranet.org, jorge.rueda@icra.it, ruffini@icra.it
[2] ICRA, Dipartimento di Fisica, Sapienza Università di Roma, P.le Aldo Moro 5, 00185 Rome, Italy
[3] INAF, Osservatorio Astronomico d'Abruzzo, Via M. Maggini snc, 64100 Teramo, Italy
[4] ICRANet-Ferrara, Dipartimento di Fisica e Scienze della Terra, Università degli Studi di Ferrara, Via Saragat 1, 44122 Ferrara, Italy
[5] Dipartimento di Fisica e Scienze della Terra, Università degli Studi di Ferrara, Via Saragat 1, 44122 Ferrara, Italy
[6] INAF, Istituto de Astrofisica e Planetologia Spaziali, Via Fosso del Cavaliere 100, 00133 Rome, Italy
[7] INAF, Viale del Parco Mellini 84, 00136 Rome, Italy

Received 18 November 2019 / Accepted 2 April 2021

ABSTRACT

A multi-decade theoretical effort has been devoted to finding an efficient mechanism to use the rotational and electr
extractable energy of a Kerr-Newman black hole (BH), to power the most energetic astrophysical sources such as gamm
(GRBs) and active galactic nuclei. We show an efficient general relativistic electrodynamical process which occurs in
engine" of a binary driven hypernova. The inner engine is composed of a rotating Kerr BH of mass M and dimensi
parameter α, a magnetic field of strength B_0 aligned and parallel to the rotation axis, and a very low-density ionized plasm
show that the gravitomagnetic interaction between the BH and the magnetic field induces an electric field that accelerat
and protons from the environment to ultrarelativistic energies emitting synchrotron radiation. We show that in GRB 1901
of mass $M = 4.4\,M_\odot$, $\alpha = 0.4$, and $B_0 \approx 4 \times 10^{10}$ G can lead to a high-energy (≥GeV) luminosity of 10^{51} erg s^{-1}. The i

The conical emission region of

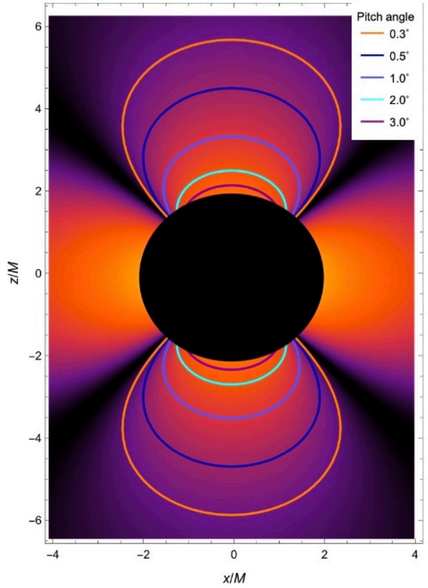

60°

Study in the undercritical E field regime

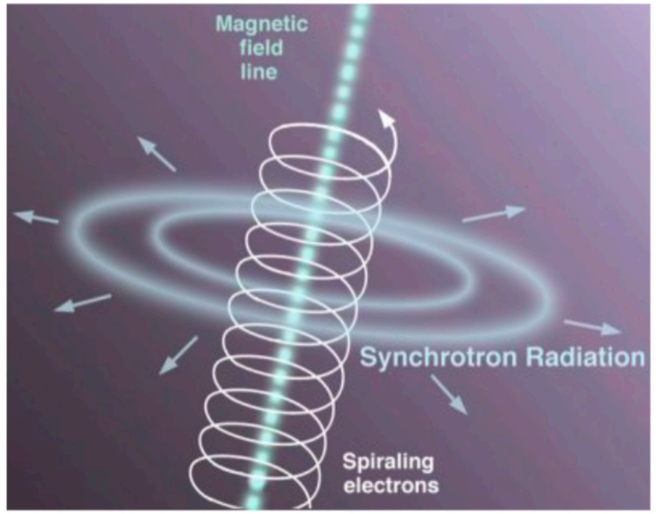

Image: Jon Lomberg/Gemini Observatory.

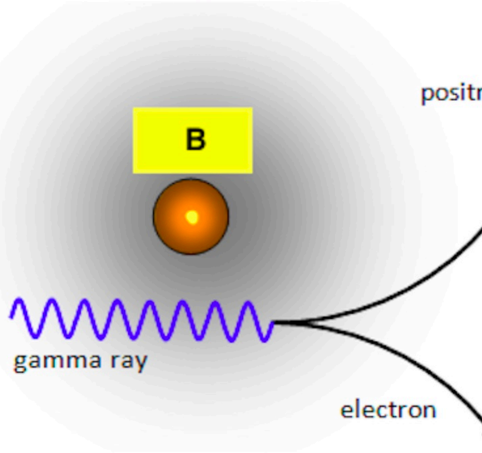

Mass, Spin and Magnetic Field

$$\mu = \left(1 - \sqrt{\frac{1+\sqrt{1-\alpha^2}}{2}}\right)^{-1} \frac{E_{\rm GeV}}{M_\odot c^2}.$$

$$\begin{aligned} E_{\rm GeV} &= E_{\rm extr}(\mu,\alpha) \\ \beta &= 3.67\times10^{-4}\alpha^{-1} \\ t_c(\langle\theta\rangle,\alpha,\beta) &= \tau_{\rm ob,1}(\mu,\alpha,\beta,L_{\rm GeV}). \end{aligned}$$

$$\begin{aligned} \beta &= \beta(\epsilon_\gamma, E_{\rm GeV}, L_{\rm GeV}, \alpha) \\ &= \frac{1}{\alpha}\left(\frac{64}{9}\sqrt{3\frac{e^2}{\hbar c}}\frac{\epsilon_\gamma}{B_c^2\, r_+(\mu,\alpha)^3}\frac{L_{\rm GeV}}{e\, B_c\, c^2}\right)^{2/7}, \end{aligned}$$

$$\beta \leq 3.67\times10^{-4}\alpha^{-1},$$

with $E_{\rm GeV} = 1.8\times10^{53}$ erg, $L_{\rm GeV} = 1.46\times10^{52}$ erg s^{-1} and photon energy $\epsilon_\gamma = 0.1$ GeV.

For the given energy and luminosity,

- $\beta = 8.9\times10^{-4}$, i.e. $B_0 \approx 3.9\times10^{10}$ G.
- $\alpha = 0.414$
- $M = 4.447\ M_\odot$
- $M_{\rm irr} = 4.346\ M_\odot$

Synchrotron photons in the 0.1 GeV–1 TeV energy band, do not produce pairs if the magnetic field is below $B_0 < 3.9\times10^{10}$ G. Therefore, this region is transparent for such photons.

Over Critical E field regime and Ultrarelativistic prompt emission phase

Dyadoregion

C. Cherubini et al PRD 79, 124002 (2009)

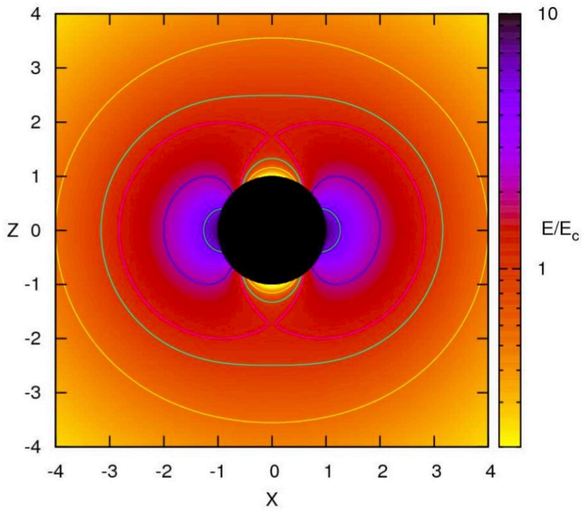

$E_c = \frac{m_e^2 c^3}{e\hbar}$ is the critical value of vacuum polarization , where m_e and e are the electron mass and charge, respectively.

GRB 190114C: UPE mechanism and inner engine

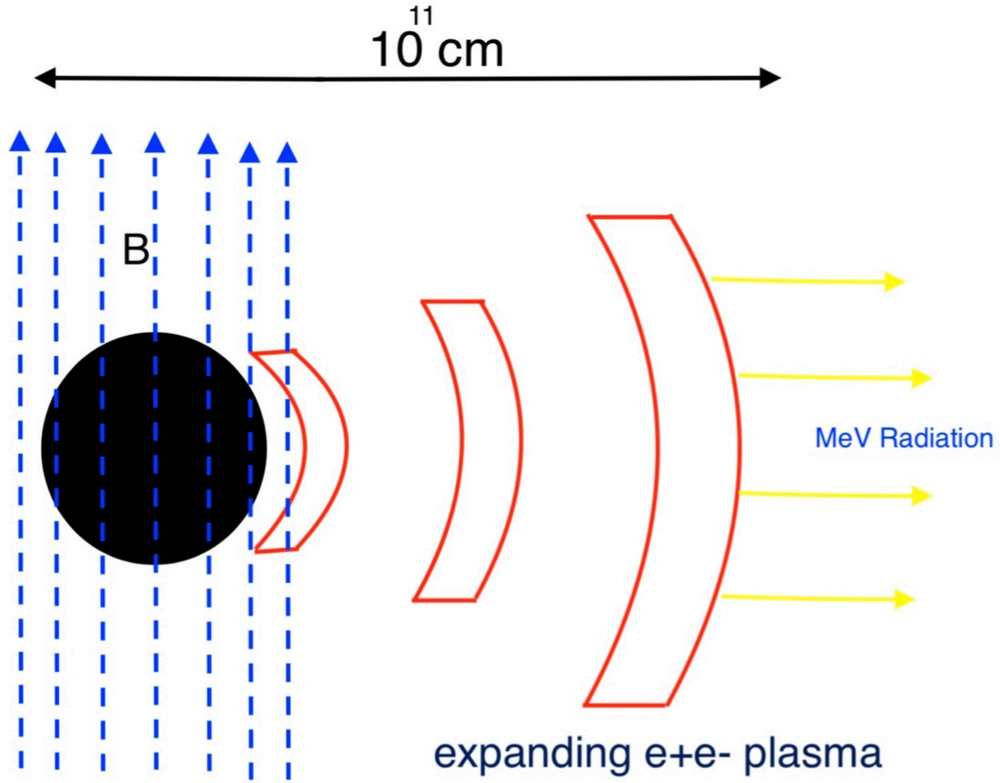

Damour and Ruffini, PRL,463 (1975)
Ruffini, Salmonson, Wilson, and Xue, A&A350, 334 (1999)
Ruffini, Salmonson, Wilson, and Xue, A&359, 855 (2000)

Nature of the ultrarelativistic prompt emission phase of GRB 190114C

R. Moradi,[1,2,3,*] J. A. Rueda,[1,2,4,5,6,†] R. Ruffini,[1,2,7,‡] Liang Li,[1,2,7,§] C. L. Bianco,[1,2,6] S. Campion,[1,2] C. Cherubini,[2,8,9] S. Filippi,[2,8,10] Y. Wang,[1,2,11,‖] and S. S. Xue[1,2]

[1]*ICRA and Dipartimento di Fisica, Università di Roma "La Sapienza", Piazzale Aldo Moro 5, I-00185 Roma, Italy*

[2]*International Center for Relativistic Astrophysics Network, Piazza della Repubblica 10, I-65122 Pescara, Italy*

[3]*INAF—Osservatorio Astronomico d'Abruzzo, Via M. Maggini snc, I-64100 Teramo, Italy*

[4]*ICRANet-Ferrara, Dipartimento di Fisica e Scienze della Terra, Università degli Studi di Ferrara, Via Saragat 1, I–44122 Ferrara, Italy*

[5]*Dipartimento di Fisica e Scienze della Terra, Università degli Studi di Ferrara, Via Saragat 1, I–44122 Ferrara, Italy*

[6]*INAF, Istituto di Astrofisica e Planetologia Spaziali, Via Fosso del Cavaliere 100, 00133 Rome, Italy*

[7]*INAF, Viale del Parco Mellini 84, 00136 Rome, Italy*

[8]*ICRA, University Campus Bio-Medico of Rome, Via Alvaro del Portillo 21, I-00128 Rome, Italy*

[9]*Department of Science and Technology for Humans and the Environment and Nonlinear Physics and Mathematical Modeling Lab, University Campus Bio-Medico of Rome, Via Alvaro del Portillo 21, 00128 Rome, Italy*

[10]*Department of Engineering, University Campus Bio-Medico of Rome, Nonlinear Physics and Mathematical Modeling Lab, Via Alvaro del Portillo 21, 00128 Rome, Italy*

[11]*INAF—Osservatorio Astronomico d'Abruzzo, Via M. Maggini snc, I-64100, Teramo, Italy*

(Received 13 May 2021; accepted 26 August 2021; published 29 September 2021)

We address the physical origin of the ultrarelativistic prompt emission (UPE) phase of GRB 190114C observed in the interval $t_{\rm rf} = 1.9$–3.99 s, by the *Fermi*-GBM in 10 keV–10 MeV energy band. Thanks to the high signal-to-noise ratio of *Fermi*-GBM data, a time-resolved spectral analysis has evidenced a sequence of similar blackbody plus cutoff power-law spectra (BB + CPL), on ever decreasing time

GRB 190114C:Ultra Relativistic Propmpt Emission Phase (UPE)

Moradi, Rueda, Ruffini, Li, et al., PRD 104, 063043 (2021).

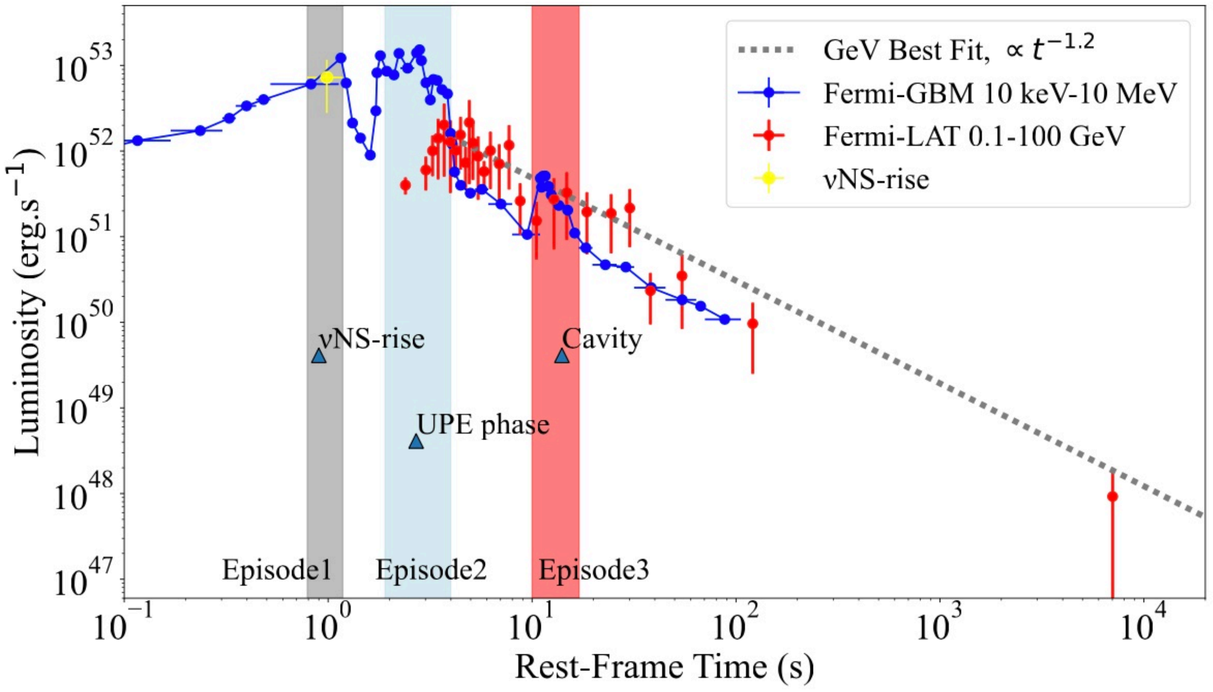

GRB 190114C: UPE phase

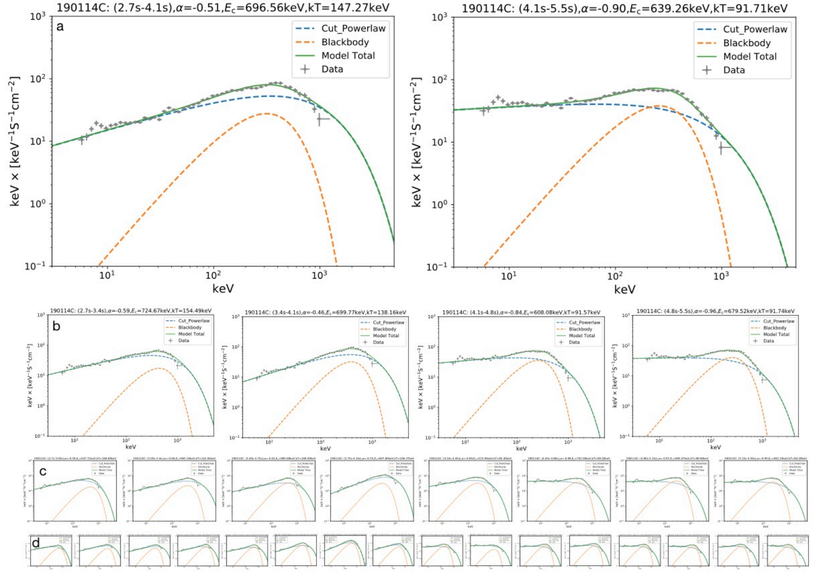

Time-resolved spectral analysis of UPE phase GRB 190114C.

GRB 190114C: UPE mechanism and inner engine

The electromagnetic field of the *inner engine* in the Carter's orthonormal tetrad is:

$$E_{\hat{r}} = \frac{\hat{a}B_0}{\Sigma}\left[r\sin^2\theta - \frac{\hat{M}\left(\cos^2\theta+1\right)\left(r^2-\hat{a}^2\cos^2\theta\right)}{\Sigma}\right], \quad (1)$$

$$E_{\hat{\theta}} = \frac{\hat{a}B_0}{\Sigma}\sin\theta\cos\theta\sqrt{\Delta}, \quad (2)$$

$$B_{\hat{r}} = -\frac{B_0\cos\theta}{\Sigma}\left[-\frac{2\hat{a}^2\hat{M}r\left(\cos^2\theta+1\right)}{\Sigma}+\hat{a}^2+r^2\right], \quad (3)$$

$$B_{\hat{\theta}} = \frac{B_0 r}{\Sigma}\sin\theta\sqrt{\Delta}, \quad (4)$$

where $\Sigma = r^2+\hat{a}^2\cos^2\theta$, $\Delta = r^2-2\hat{M}r+\hat{a}^2$, $\hat{M} = GM/c^2$, $\hat{a} = a/c = J/(Mc)$, being M and J the mass and angular momentum of the Kerr BH. The (outer) event horizon is located at $r_+ = (\hat{M}+\sqrt{\hat{M}^2-\hat{a}^2})$.

Analogy with Kerr-Newmann

Dyadoregion

The dyadoregion energy:

$$
\begin{aligned}
E_{(r_+,r_{\rm d})} &= \frac{(2B_0JG/c^3)^2}{4r_+}\left(1-\frac{r_+}{r_{\rm d}}\right)+\frac{(2B_0JG/c^3)^2}{4\hat{a}} \\
&\times \left[\left(1+\frac{\hat{a}^2}{r_+^2}\right)\arctan\left(\frac{\hat{a}}{r_+}\right)\right. \\
&- \left.\left(1+\frac{\hat{a}^2}{r_d^2}\right)\arctan\left(\frac{\hat{a}}{r_d}\right)\right], \qquad (5)
\end{aligned}
$$

where r_d is the radius of the dyadoregion

$$
\left(\frac{r_d}{\hat{M}}\right)^2=\frac{1}{2}\frac{\lambda}{\mu\epsilon}-\alpha^2+\left(\frac{1}{4}\frac{\lambda^2}{\mu^2\epsilon^2}-2\frac{\lambda}{\mu\epsilon}\alpha^2\right)^{1/2} \qquad (6)
$$

with $\epsilon = E_c M_\odot G^{3/2}/c^4 \approx 1.873\times10^{-6}$, and

$$
\lambda=(2B_0JG/c^3)/(\sqrt{G}M), \qquad (7)
$$

is the effective charge-to-mass ratio.
The characteristic width of the dyadoregion, which demonstrates the region in which the electric field around the BH is overctitical is

$$
\Delta_{\rm d}(t)=r_d(t)-r_+(t). \qquad (8)
$$

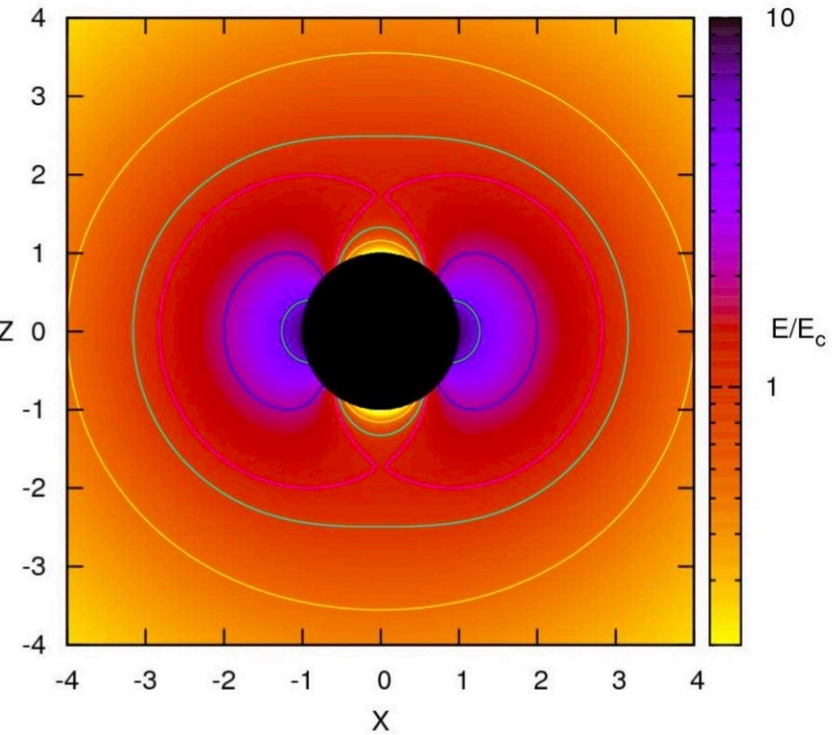

key parameters for calculating the transparency radius of each impulse are:

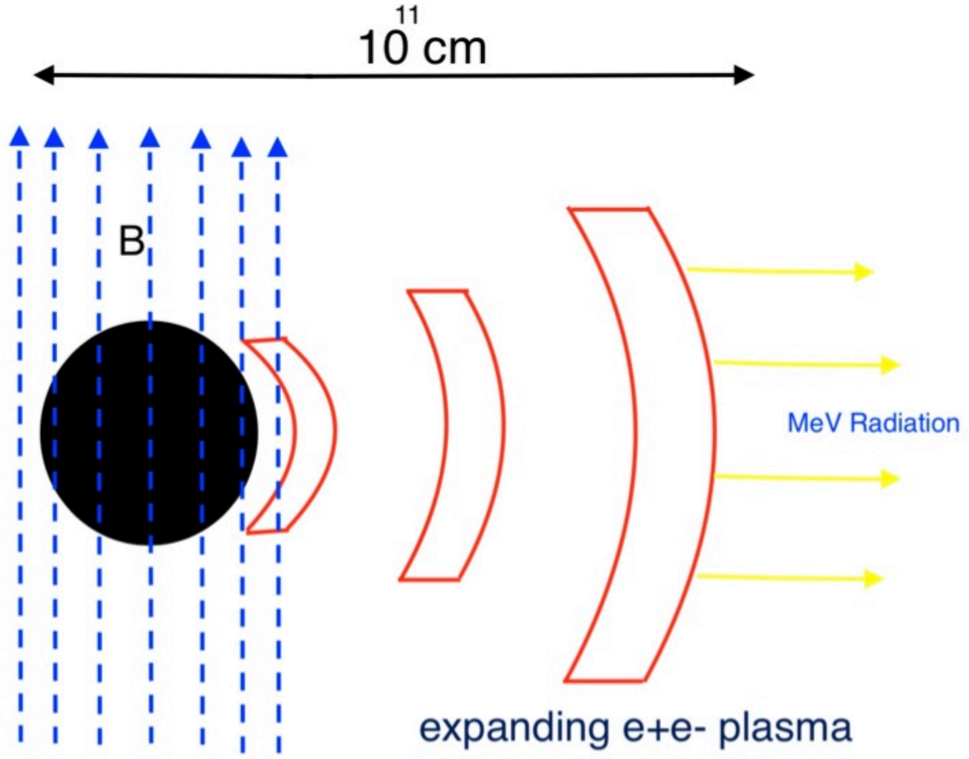

- its isotropic energy, $E_{\rm iso}$,
- its ratio of black body energy to isotropic energy ($E^{\rm obs}_{\rm P-GRB}/E_{\rm iso}$)
- its value of black body temperature in keV, ($T_{\rm obs}$)
- its width $\Delta_{\rm lab} = \Delta_{\rm d}$.

Transparency obtained from the lower limit of magnetic field, $B_0 = 2.3 \times 10^{14}$ G ($|\mathbf{E}| = E_c$ at the end of UPE phase).

Not Continuous Emission But A discrete emission with time scale of 10^-9 s

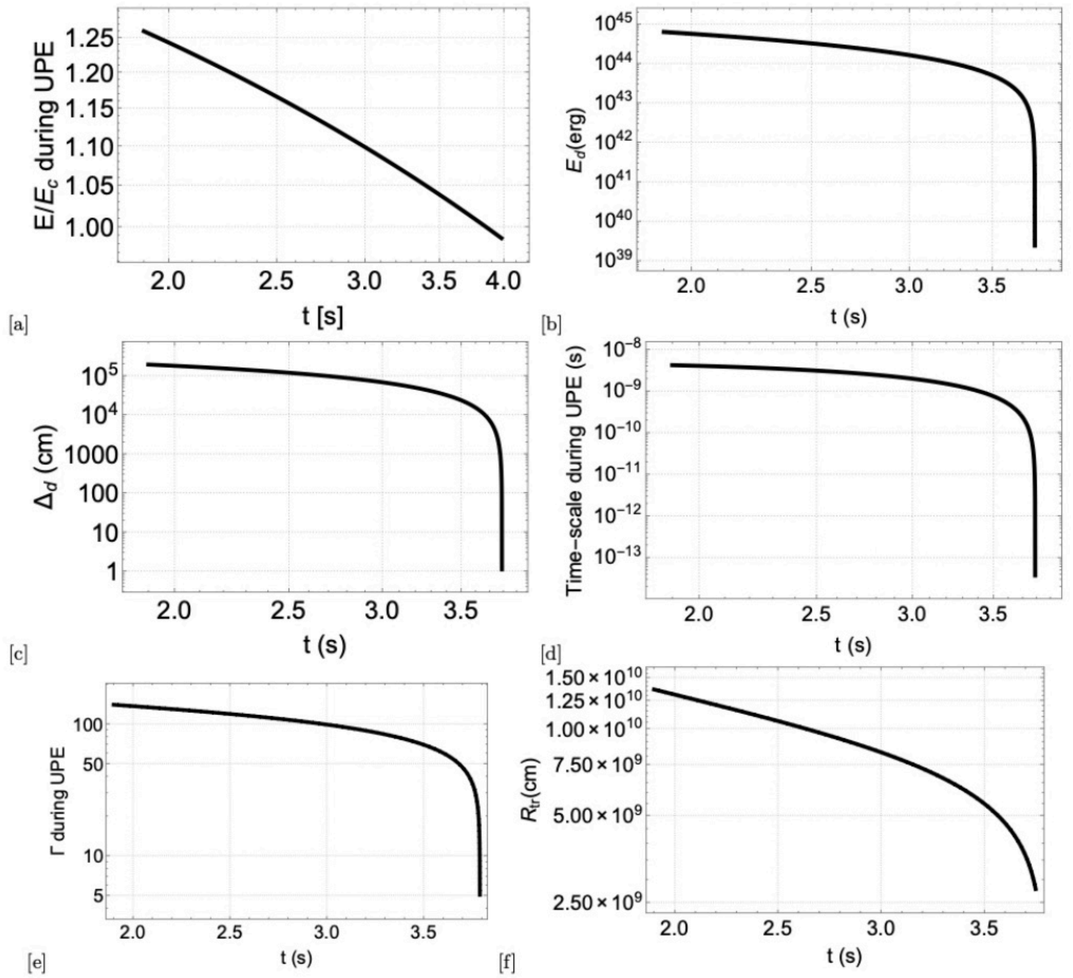

GRB 180720B
Rastegarnia et al in prepsration

iii

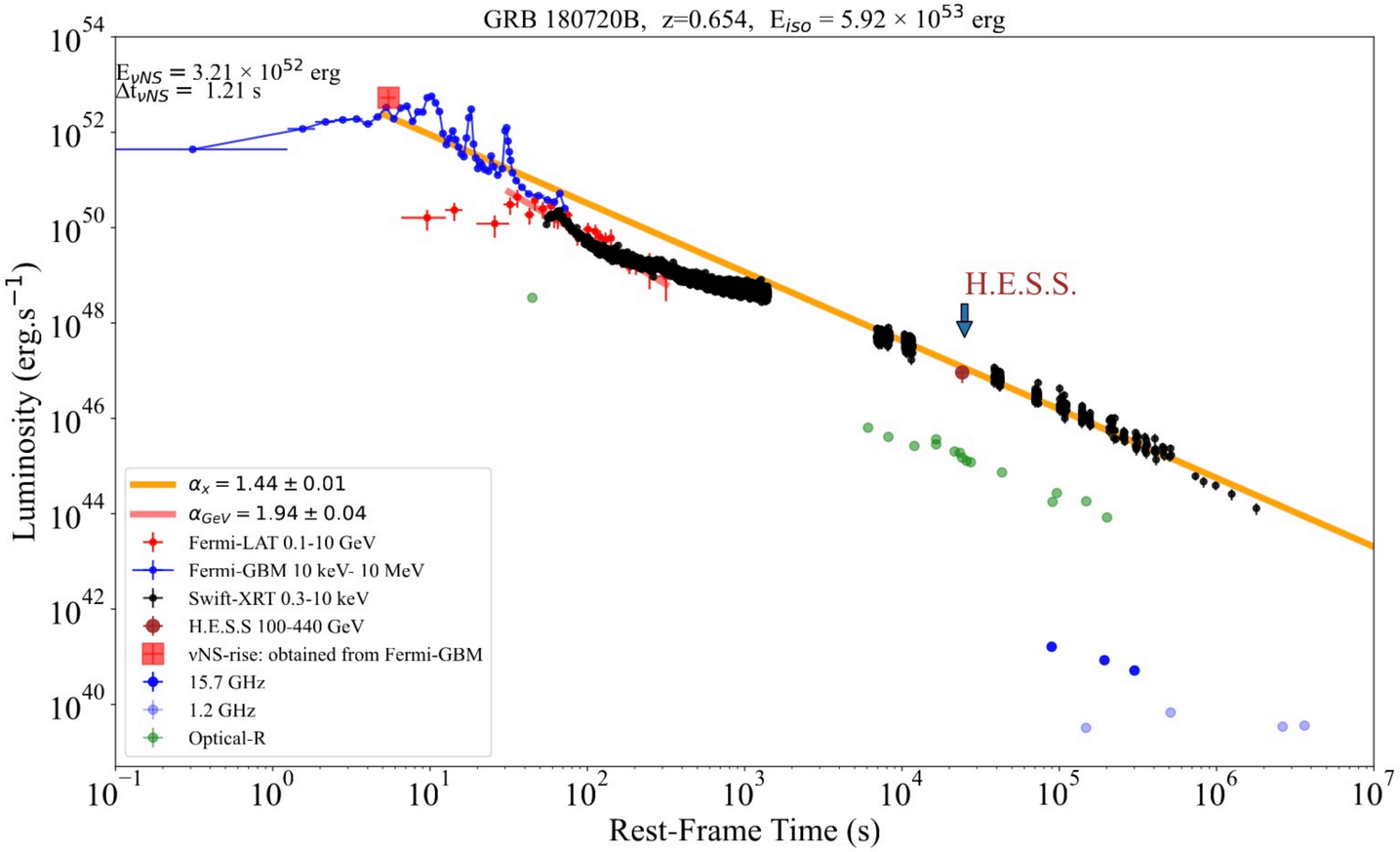

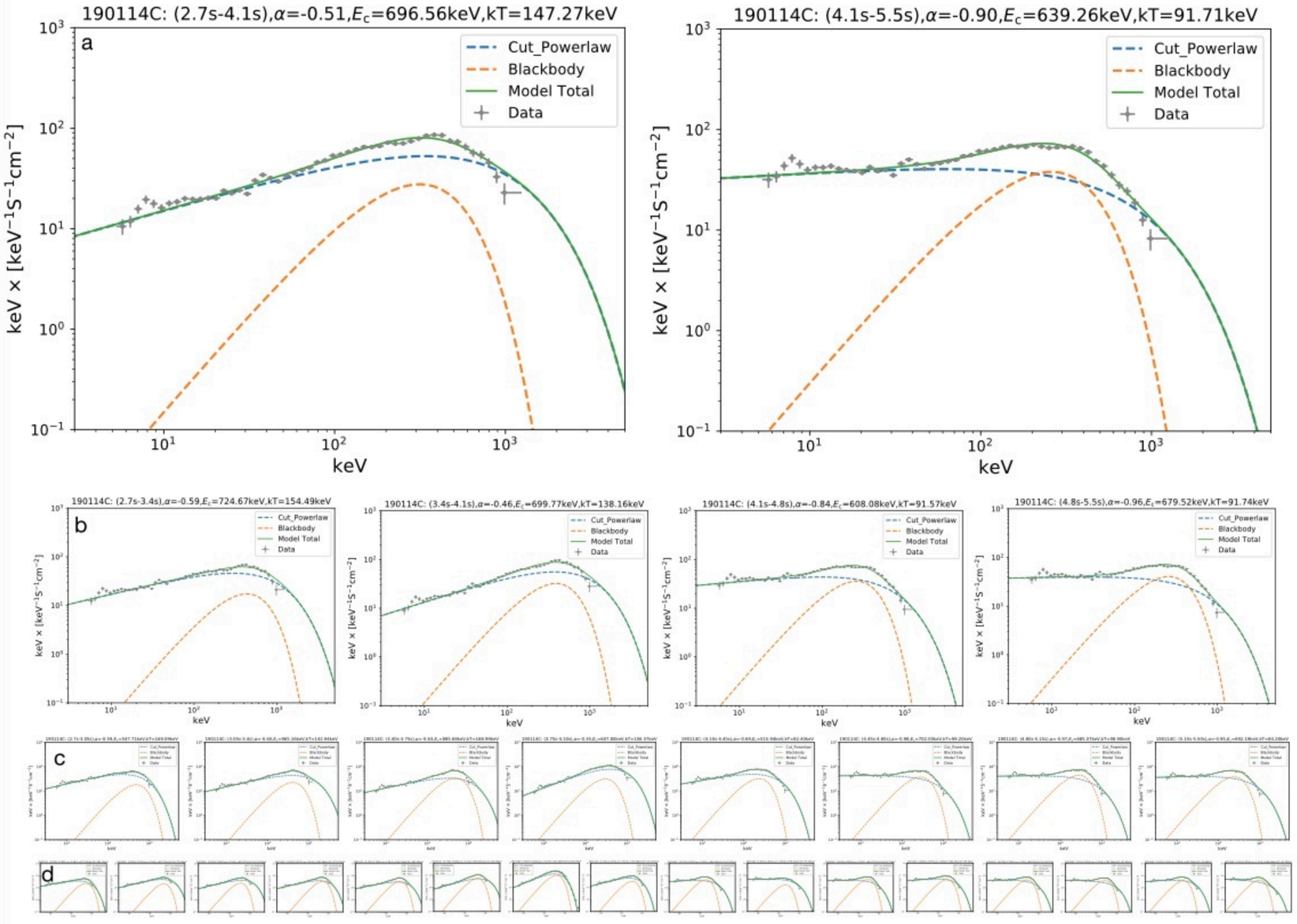
190114C: (2.7s-4.1s),α=-0.51,E_c=696.56keV,kT=147.27keV
190114C: (4.1s-5.5s),α=-0.90,E_c=639.26keV,kT=91.71keV
a
b
c
d
Cut_Powerlaw
Blackbody
Model Total
Data
keV
keV × [keV⁻¹S⁻¹cm⁻²]
190114C: (2.7s-3.4s),α=-0.59,E_c=724.67keV,kT=154.49keV
190114C: (3.4s-4.1s),α=-0.46,E_c=699.77keV,kT=138.16keV
190114C: (4.1s-4.8s),α=-0.84,E_c=608.08keV,kT=91.57keV
190114C: (4.8s-5.5s),α=-0.96,E_c=679.52keV,kT=91.74keV

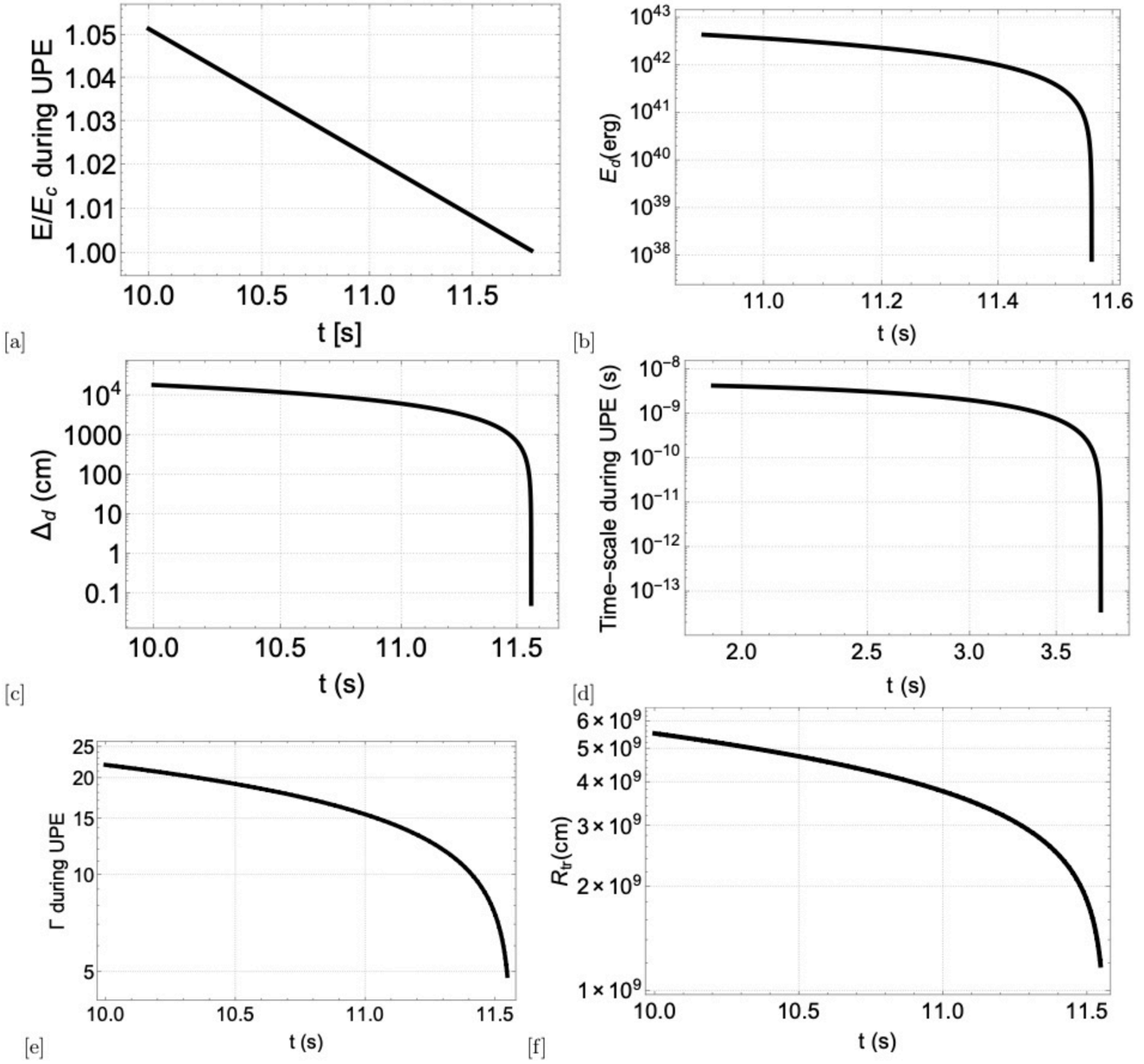
E/E_c during UPE
1.05
1.04
1.03
1.02
1.01
1.00
10.0
10.5
11.0
11.5
t [s]
[a]
E_d(erg)
10^43
10^42
10^41
10^40
10^39
10^38
11.0
11.2
11.4
11.6
t (s)
[b]
Δ_d (cm)
10^4
1000
100
10
1
0.1
10.0
10.5
11.0
11.5
t (s)
[c]
Time−scale during UPE (s)
10^−8
10^−9
10^−10
10^−11
10^−12
10^−13
2.0
2.5
3.0
3.5
t (s)
[d]
Γ during UPE
25
20
15
10
5
10.0
10.5
11.0
11.5
t (s)
[e]
R_tr(cm)
6×10^9
5×10^9
4×10^9
3×10^9
2×10^9
1×10^9
10.0
10.5
11.0
11.5
t (s)
[f]

What are we learning on BHs from GRB observations?

The usual assumptions adopted for mathematical convenience in the description of the Kerr BH are:

1. The condition of the stationary space-time.
2. The condition of the vacuum space-time.
3. The condition of asymptotic flatness.

From the observation of GRBs (see e.g. GRB 1807820B and GRB 190114C) we conclude that Kerr BHs in these systems are:

1. are endowed with a magnetic field, B_0 parallel to their rotation axis;
2. They have no electric charge and the gravitomagnetic interaction between the BH angular momentum (J) and the surrounding magnetic field (B_0) induces an electric field which can be viewed as produced by an effective charge $Q_{\rm eff} = 2J\,B_0$ (Papapetrou-Wald solution);
3. They are embedded in a low density fully ionized plasma, essential for the electrodynamics of the energy extraction process (Ruffini, et al., 2019, ApJ 883, 191).

What are we learning on BHs from GRB observations?

Thanks to “the extractable energy” in the Christodoulou-Ruffini mass-energy formula, the Kerr BHs (Ruffini, et al., 2019, ApJ 886, 82):

1. radiate in principle for an infinite time; they follow a power-law luminosity in the source rest-frame $L_{\rm GeV} = A_{\rm GeV} t^{-\alpha_{\rm GeV}}$ (Ruffini, et al., 2021, MNRAS 504, 5301);
2. radiate GeV photons in a conical region of 60° around the BH rotation axis;
3. they do not emit continuously but in blackholic quanta (Rueda & Ruffini, 2020, EPJC 80, 300);

All the above applies not only to GRBs but also to AGN scaling the BH from $\sim 10 M_\odot$ to $10^9 M_\odot$.